https://doi.org/10.1007/s41230-021-0117-8

Microstructures and tensile properties of as-cast Mg-5Sn-1Si magnesium alloy modified with trace elements of Y, Bi, Sb and Sr

He-shuai Yu[1,2], *Xue-feng Guo[1,2], Hong-bao Cui[1,2]

1. School of Materials Science and Engineering, Henan Polytechnic University, Jiaozuo 454000, Henan, China

2. Henan International Joint Research Laboratory for High-Performance Light Metallic Materials and Numerical Simulations, Henan Polytechnic University, Jiaozuo 454000, Henan, China

Abstract: The microstructures and mechanical properties of as-cast Mg-5Sn-1Si magnesium alloy modified with trace elements Y, Bi, Sb and Sr were investigated and compared. Results show that the microstructure of the as-cast Mg-5Sn-1Si alloy consists of α-Mg, Mg_2Si, Mg_2Sn and $Mg_2(Si_xSn_{1-x})$ phases. After adding 0.8wt.% Y, 0.3wt.% Bi, 0.9wt.% Sb and 0.9wt.% Sr, respectively into the Mg-5Sn-1Si magnesium alloy, $Mg_{24}Y_5$, Mg_3Bi_2, Mg_3Sb_2 and Mg_2Sr phases are precipitated accordingly. Trace elements can refine α-Mg grain and Chinese script-shaped Mg_2Si phase. Refinement efficiency of different trace elements on α-Mg grain and Mg_2Si phase is varied. Sr element has the best refinement effect, followed by Sb and Bi, while Y has the least refinement effect. Mg-5Sn-1Si-0.9Sr alloy has higher tensile properties than the other three modified alloys. The refinement mechanism of Y, Bi and Sr elements on Mg-5Sn-1Si magnesium alloy can be explained by the growth restriction factors and the solute undercooling. For Mg-5Sn-1Si-0.9Sb alloy, the heterogeneous nuclei of Mg_3Sb_2 phase is the main reason for the refinement of grains and second phases.

Key words: magnesium alloy; Mg-5Sn-1Si alloy; Y, Bi, Sb, Sr; Mg_2Si phase

CLC numbers: TG146.22 **Document code:** A **Article ID:** 1672-6421(2021)01-009-09

1 Introduction

As the lightest metallic engineering materials, magnesium alloys have received a great attention in recent years due to their several advantages such as high strength-to-weight ratio, high thermal conductivity, high dimensional stability, good electromagnetic shielding characteristics, high damping capacity and good machineability [1-3]. However, commercial cast magnesium alloys such as AZ and AM alloys are limited in some applications because of their poor creep resistances and mechanical properties at elevated temperatures over 120 °C. This is caused by the low-melting-point of $Mg_{17}Al_{12}$ phase which precipitates at grain boundaries during solidification [4-6]. Hence, in the last decade, improving elevated temperature properties of magnesium alloys has become a critical issue. In order to overcome or minimize the deterioration of $Mg_{17}Al_{12}$ phase on high-temperature mechanical properties, new alloys were developed and investigated, for example, Mg-Al-RE [7], Mg-Zn-Y-Ce [8, 9], Mg-Sn-Ca [10] and Mg-Gd [11] system alloys. It was found that Mg-Si based alloys are potentially elevated temperature magnesium alloys because Mg_2Si phase in Mg-Si based alloys has high melting point, high hardness, low density (similar to Mg alloy), high elastic modulus and low thermal expansion coefficient. Moreover, Mg_2Si phase is very stable and can impede grain boundary sliding at elevated temperatures [12-14]. Whereas, under low solidification rates, Mg_2Si phase precipitates from Mg-Si-based melt in a coarse Chinese script-shaped form, which has proved to be very damaging to the mechanical properties of the alloys. The reasons for deteriorating mechanical properties of the Mg-Si alloys are related to the sharp corners and the brittleness of the coarse Mg_2Si compound, as well as the poor α-Mg/Mg_2Si interfacial adhesion[15]. Therefore, modifying and refining Mg_2Si phase, and improving the α-Mg/Mg_2Si interfacial adhesion are thought to be the key factors to enhance the mechanical properties of Mg-Si based alloys.

***Xue-feng Guo**

Male, born in 1962, Professor. He is mainly engaged in the research and development of microstructure and properties of heat-resistant magnesium alloys, rapidly solidified magnesium alloys and deformed magnesium alloys. To date, he has published 4 books and more than 200 papers.

E-mail: guoxuef@hpu.edu.cn;

Received: 2020-08-21; Accepted: 2020-10-28

At present, there are many ways to enhance the strength of magnesium alloys at room and high temperatures, in which the most fundamental and effective methods are element alloying and deformation [16]. Alloying elements such as Sr [17, 18], P [19], Bi [20], Y [21], Sb [22-24], La [25], Nd [26], Gd [27] and compound KBF_4 [28] have positive modification effects on the morphology of Mg_2Si phase. In general, trace alloying elements only change the morphologies of the constituent phases during solidification, and cannot change their inherent structures. Therefore, adding trace elements to Mg-Si alloys is considered a useful method to modify and refine the morphology of Mg_2Si phase. Considering that Si, Ge, Sn and Pb belong to the same group, i.e. IVA group, and that they all can form the same anti-CaF_2 crystal structure Mg_2X (X=Si, Ge, Sn or Pb) with magnesium, the Mg_2X is considered a linear compound with an Fm-3m space group. These Mg_2X compounds may have certain solubility to each other, as is known, Mg_2Si and Mg_2Sn have certain solubility to each other at least. Thus, the mechanical properties and α-Mg/Mg_2X interfacial adhesion of the alloys could be changed whether being improved or deteriorated. It has been revealed that Mg_2Si and Mg_2Sn have almost the same lattice constants (Mg_2Si is 0.633 nm, Mg_2Sn is 0.699 nm) and have some solubility to each other by Sn and Si replacement to each other. Mg_2Sn phase can dissolve 3at.%–14at.% Si, Mg_2Si can dissolve 2at.%–13.3at.% Sn. Wang's [15] calculations indicate that a new reinforcement phase $Mg_2(Si_xSn_{1-x})$ forms by a substitution reaction in the Mg-Si-Sn alloys, and there are a certain percentage of covalent bonds in $Mg_2(Si_xSn_{1-x})$, which ensure $Mg_2(Si_xSn_{1-x})$ has sufficient hardness to act as a reinforcement phase and exhibits greater ductility than that of the unalloyed Mg_2Si phase. If some Sn atoms replace equivalent Si atoms from Mg_2Si phase, the value of interfacial adhesion work (Wad) between α-Mg matrix and the $Mg_2(Si_xSn_{1-x})$ compound increases, then, the poor interfacial adhesion between α-Mg and unalloyed Mg_2Si phase is improved. Hence, it is reasonable to speculate that simultaneously adding Sn and other trace elements to Mg-Si alloys can improve the mechanical properties of the Mg-Si alloys. Accordingly, selecting suitable trace elements which can modify and refine the morphology of Mg_2Si phase in Mg-Sn-Si based alloy appears to be very important for further research.

Liu et al. [29] studied the microstructures, tensile properties, and creep behaviour of as-cast Mg-(1–10)wt.% Sn alloys, and found that Mg-5wt.% Sn alloy has the best mechanical performance at room and elevated temperatures. Jiang et al. [21] studied the effect of Y on modification of Mg_2Si in Mg-Si alloys and indicated that when the Y content is 0.1wt.% or 0.4wt.%, the sizes of primary and eutectic Mg_2Si do not significantly reduce. When the Y content is 0.8wt.%, the mean size of Mg_2Si particles decreases from more than 100 μm to about 30 μm or less; however, with the further increase of the Y content to 1.2wt.%, the primary Mg_2Si becomes coarser again and even larger than that in the unmodified alloy. Ma et al.[30] investigated the influence of trace Y element on the microstructure of Mg-5Sn-1Si alloy and found that when the Y content is 0.8wt.%, the modification effect of Y on the microstructure of the alloy is excellent. Guo et al. [20] studied the modification of Mg_2Si morphology in Mg-Si alloys with Bi element and found that the optimal modification effect is obtained when the Bi content is no more than 0.5wt.%. Yan et al. [31] researched the influence of Sb modification on microstructure and mechanical properties of Mg_2Si/AM60 composite and indicated that Mg_3Sb_2 can promote the formation of fine polygonal type Mg_2Si by providing a nucleation site, and the ultimate tensile strength is enhanced by 12.2% with the addition of 0.8wt.% Sb. Wang et al.[32] proved that after adding 0.9wt.% Sb into Mg-5Sn-1Si alloy, the arm spacing of Mg_2Si phase is decreased. Cong et al.[33] investigated the effect of Sr on microstructure of as-cast Mg-6Zn-4Si alloy and found that the grain size of the primary Mg_2Si decreased initially and then gradually increased with increasing Sr amount, and the optimal mechanical properties and wear resistance could be obtained by a Sr addition of 0.5wt.%.

Based on the above discussion and published research results, in this present work, the effects of trace elements: 0.8wt.% Y, 0.3wt.% Bi, 0.9wt.% Sb and 0.9wt.% Sr on microstructure and mechanical properties of cast Mg-5Sn-1Si magnesium alloy were investigated, and the modification and refinement results of α-Mg grain and Mg_2Si phase were compared.

2 Experimental procedure

The nominal compositions of Mg-5Sn-1Si based alloys used in this study are presented in Table 1. The investigated materials were prepared with a resistance furnace by melting pure Mg (>99.90%), Sn (>99.99%), Bi (>99.99%), Sb (>99.99%) and master alloys of Mg-5.0% Si, Mg-10% Sr and Mg-30.0% Y in a steel crucible. Before melting, all of the raw materials were preheated to 120 °C to remove the surface moisture. The pure Mg ingots were firstly put into the steel crucible and heated to 720 °C with protection of mixture gas of 0.5vol.% SF6 and 99.5vol.% CO_2. When the pure Mg ingots were completely melted, the preheated Sn, Bi, Sb, Mg-30.0% Y, Mg-10% Sr and Mg-5.0% Si master alloys were respectively added into the Mg melt. Then the temperature was raised to 780 °C and held for 30 min to ensure the Mg-5.0% Si master alloy being completely melted. During holding period, the melts were stirred with a carbon bar for several times in order to melt the Mg-5.0% Si master alloy completely and make the compositions of the melts uniform. Then, the melts were cast into ingots with a diameter of 105 mm and a length of 450 mm. In order to analyze the microstructures of the alloys, the as-cast metallographic samples were prepared in accordance with the standard routines and etched with picric acid solution (5 g picric acid + 10 mL glacial acetic +10 mL distilled water +80 mL anhydrous ethanol) for 5–10 s at room temperature. Microstructural analysis was conducted by using an optical microscope (OM, Olympus GX51) and a scanning electron microscope (SEM, JSM-6700F) equipped with an energy dispersive X-ray spectrometer (Oxford, Germany). The phases of the alloys were analyzed by using X-Ray diffraction (XRD, Rigaku D/max-3C type,

Japan), the radiation source was Cu Kα, scanning step and range were 0.033° and 10°–90°, respectively. Thermal analysis by differential scanning calorimetry (DSC) were performed using a NETZSCH STA 2500 system. For the DSC tests, samples weighed around 20 mg were heated under flowing argon atmosphere from room temperature to 750 °C. The heating curves were recorded at a controlling speed of 5 °C·min^{-1}. The tensile properties at room temperature were determined from the stress-strain curves. The 0.2% yield strength (YS), ultimate tensile strength (UTS) and elongation to failure were obtained based on the average results of three valid tests.

Table 1: Nominal compositions of experimental Mg-5Sn-1Si alloys (wt.%)

Alloys	Sn	Si	Y	Bi	Sb	Sr	Mg
1	5.30	1.32	-	-	-	-	Bal.
2	5.39	1.36	0.81	-	-	-	Bal.
3	5.35	1.37	-	0.32	-	-	Bal.
4	5.32	1.34	-	-	0.88	-	Bal.
5	5.38	1.35	-	-	-	0.89	Bal.

3 Results and discussion

3.1 Microstructure of as-cast Mg-5Sn-1Si alloy

Figure 1 presents the XRD pattern of the Mg-5Sn-1Si alloy. It indicates that this alloy consists of α-Mg, Mg_2Si and Mg_2Sn phases. The corresponding SEM images of the as-cast Mg-5Sn-1Si alloy are presented in Fig. 2. It can be observed that the matrix of the alloy is α-Mg solid solution and the others are secondary phases with different morphologies which spread on the matrix and inter-dendritic regions. The inter-dendrite compounds have two morphologies: one is in Chinese script and another in irregular-shape which is abnormal eutectic phase. Combining the EDS (Table 2) and XRD results, it can be proved that the abnormal eutectic compounds (Point l in Fig. 2) which enrich in Mg and Sn and minor Si elements are Mg_2Sn phase. The compound in Chinese script morphology which locates at the grain boundary has the typical characteristics of Mg_2Si phase. EDS results show that the compound at the boundries of Mg_2Si phase is much different from the main part of the Mg_2Si. It contains a certain amount of Sn element, so it is a new phase $Mg_2(Si_xSn_{1-x})$. Therefore, the as-cast Mg-5Sn-1Si alloy consists of α-Mg, abnormal eutectic Mg_2Sn phase, Chinese-character Mg_2Si phase at grain boundaries, and some ternary $Mg_2(Si_xSn_{1-x})$ compounds as well. The ternary $Mg_2(Si_xSn_{1-x})$ compound is at the boundaries of the Mg_2Si phase. Under low solidification rate, the Mg_2Si phase tends to grow into the Chinese script form in Mg-5Sn-1Si alloy, which is detrimental to the mechanical properties of the alloys.

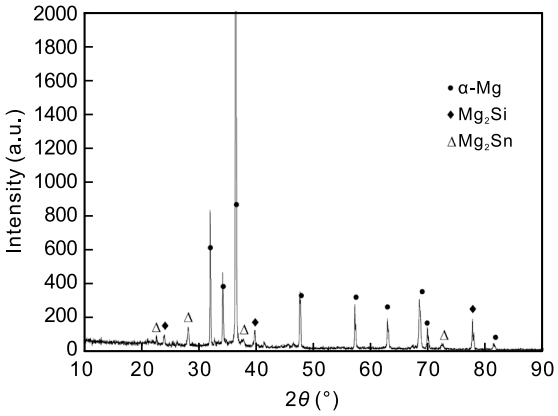

Fig. 1: XRD pattern of as-cast Mg-5Sn-1Si alloy

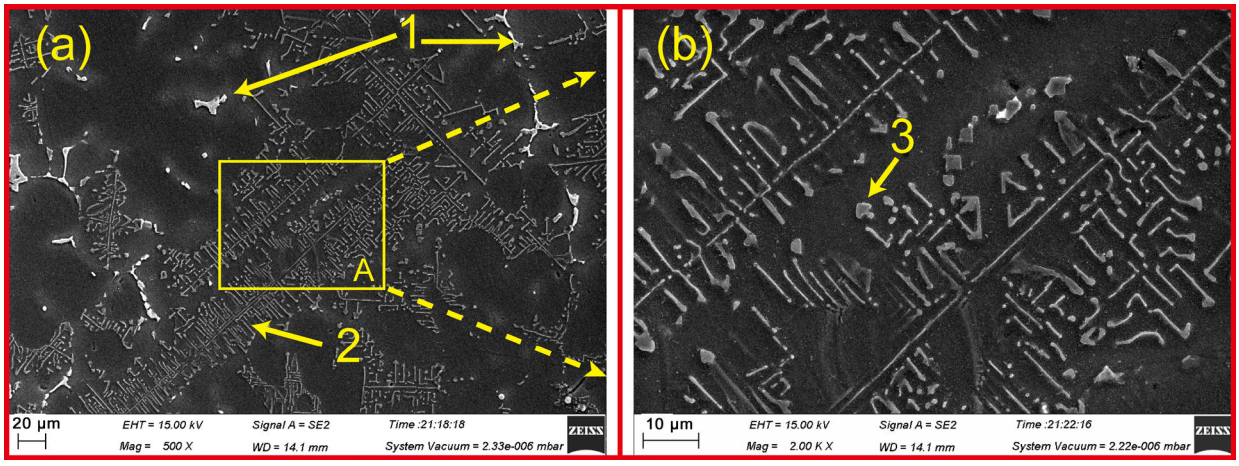

Fig. 2: (a) SEM images of as-cast Mg-5Sn-1Si alloy; (b) SEM image with higher magnification of Zone A in (a)

Table 2: EDS results of phases in as-cast Mg-5Sn-1Si alloy (wt.%)

Points in Fig. 2	Mg	Sn	Si
1	34.12	63.99	1.89
2	59.38	11.47	29.15
3	82.73	6.12	11.15

3.2 Microstructures of modified Mg-5Sn-1Si magnesium alloys

Figure 3 shows the XRD results of the modified Mg-5Sn-1Si magnesium alloys. It can be found that after adding 0.8wt.% Y, 0.3wt.% Bi, 0.9wt.% Sb and 0.9wt.% Sr, respectively, to the Mg-5Sn-1Si alloy, except the α-Mg, Mg_2Si, Mg_2Sn and $Mg_2(Si_xSn_{1-x})$ phases, $Mg_{24}Y_5$, Mg_3Bi_2, Mg_3Sb_2 and Mg_2Sr phases, respectively, were found. The OM images of the modified Mg-5Sn-1Si magnesium alloys are shown in Fig. 4 and the corresponding SEM images are shown in Fig. 5. The phase compositions measured with EDS are given in Table 3. This indicates that trace elements can not only change the phase morphology but also influence the phase formation in the modified Mg-5Sn-1Si magnesium alloys.

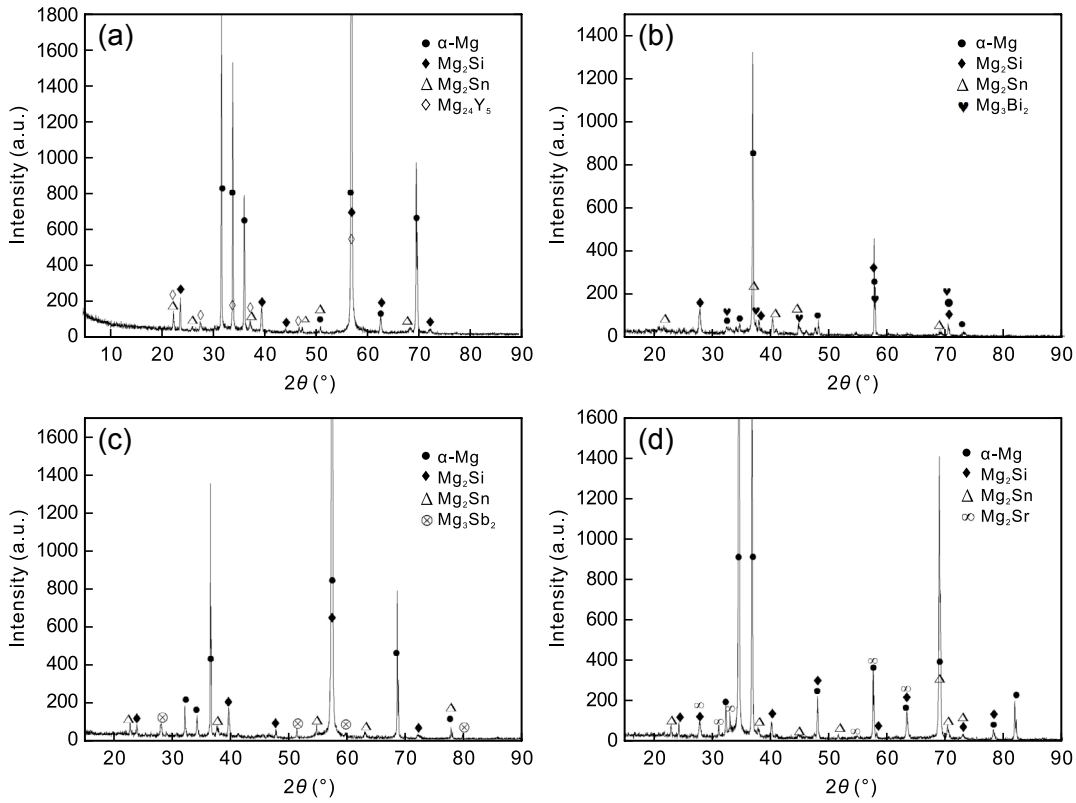

Fig. 3: XRD patterns of modified Mg-5Sn-1Si alloys with 0.8wt.% Y (a), 0.3wt.% Bi (b), 0.9wt.% Sb (c), and 0.9wt.% Sr (d)

After adding trace elements to Mg-5Sn-1Si alloy, the microstructures are changed obviously: the matrix grain sizes of the modified alloys are refined. For the Mg-5Sn-1Si alloys modified with 0.8wt.% Y, 0.3wt.% Bi, 0.9wt.% Sb, and 0.9wt.% Sr, their α-Mg grain sizes are refined from the unmodified 135 μm to about 105 μm, 97 μm, 94 μm and 74 μm, respectively. Meanwhile, the morphology of Mg_2Si phase in the modified alloys is also different from the unmodified one, although the refinement efficiency on Mg_2Si phase is different with different trace elements. Figure 4(a) and Fig. 5(a) show the microstructures of Mg-5Sn-1Si-0.8Y alloy. Almost all the Mg_2Si phases are refined from the previous coarse Chinese script [Fig. 1(a)] into a discontinuous network spread on the matrix. The similar phenomenon can also be found in Mg-5Sn-1Si-0.3Bi alloy, as shown in Fig. 4(b) and Fig. 5(b). The dendritic arm spacing of Mg_2Si phase is smaller in Mg-5Sn-1Si-0.3Bi alloy than that in Mg-5Sn-1Si-0.8Y alloy. This means the refinement efficiency of Bi on Mg_2Si is better than that of Y. By adding trace Sb into Mg-5Sn-1Si, the massive Mg_2Si phase is refined and the coarse Chinese script Mg_2Si is broken into islands and dispersed at the grain boundaries. For Mg-5Sn-1Si-0.9Sb alloy, an obvious white phase marked as I in Fig. 5(c) can be identified in Mg_2Si phase. Combining Fig. 3(c) and EDS results in Table 3, it can be concluded that Phase I in Fig. 5(c) is Mg_3Sb_2, which is the nucleus of Mg_2Si. Hence, the reason for the modification and refinement of Mg_2Si phase in Mg-5Sn-1Si-0.9Sb alloy is strongly related to the heterogeneous nucleation. Meanwhile, the morphology of Mg_2Si phase in Mg-5Sn-1Si-0.9Sb alloy is much finer than that in Mg-5Sn-1Si-0.3Bi alloy. This implies that the modified effect of Sb on Mg_2Si phase is greater than that of Bi. For the Sr alloyed system, the initial Chinese script Mg_2Si is refined into very fine dendrite shapes distributed on the matrix. This indicates that Sr has very good refinement effect on Mg_2Si phase. Comparing the modification effects of the alloys, Sr has the best refinement effect compared with Sb, Bi and Y elements. Hence, the refinement efficiency sequence of trace elements on magnesium matrix and Mg_2Si compound in Mg-5Sn-1Si alloy is Sr, followed by Sb, Bi and Y.

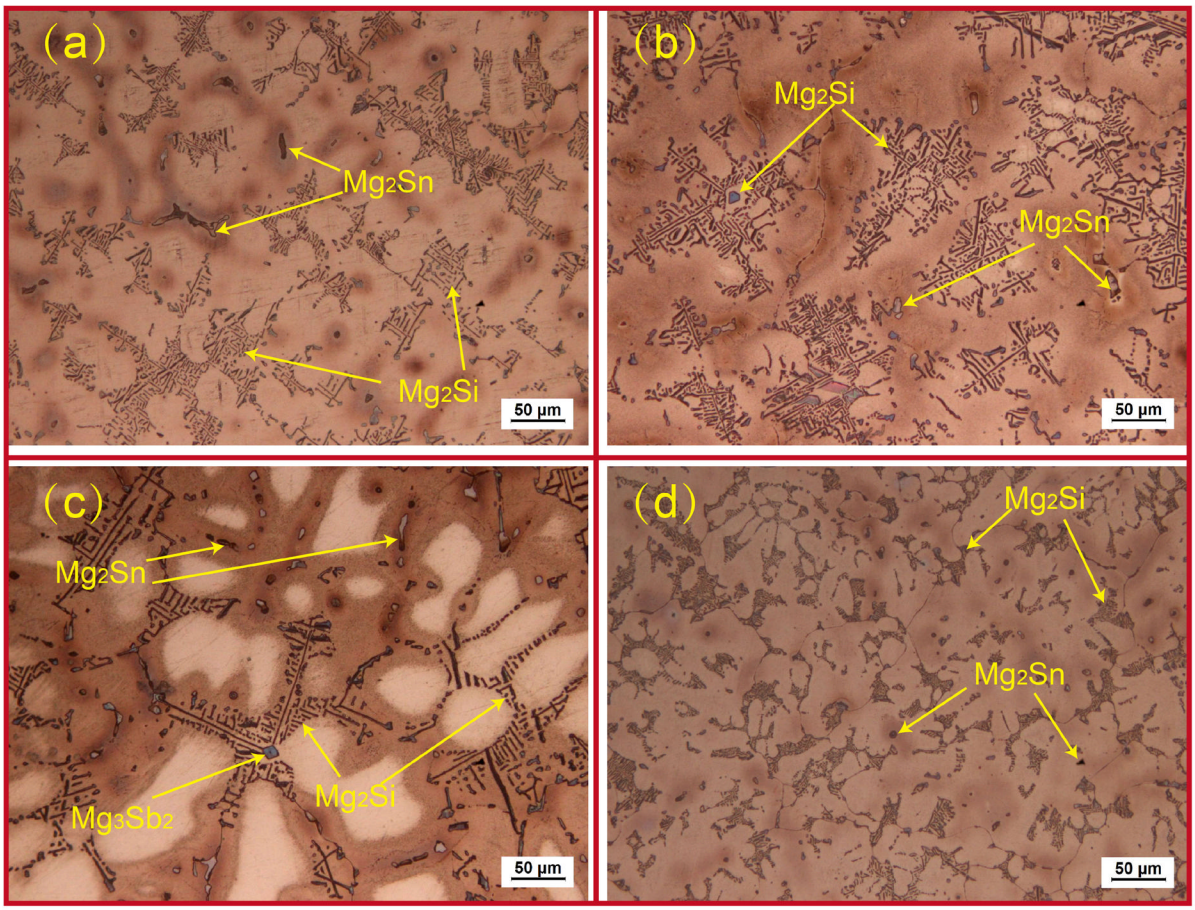

Fig. 4: Optical micrographs of as-cast Mg-5Sn-1Si alloys with 0.8wt.% Y (a), 0.3wt.% Bi (b), 0.9wt.% Sb (c), and 0.9wt.% Sr (d)

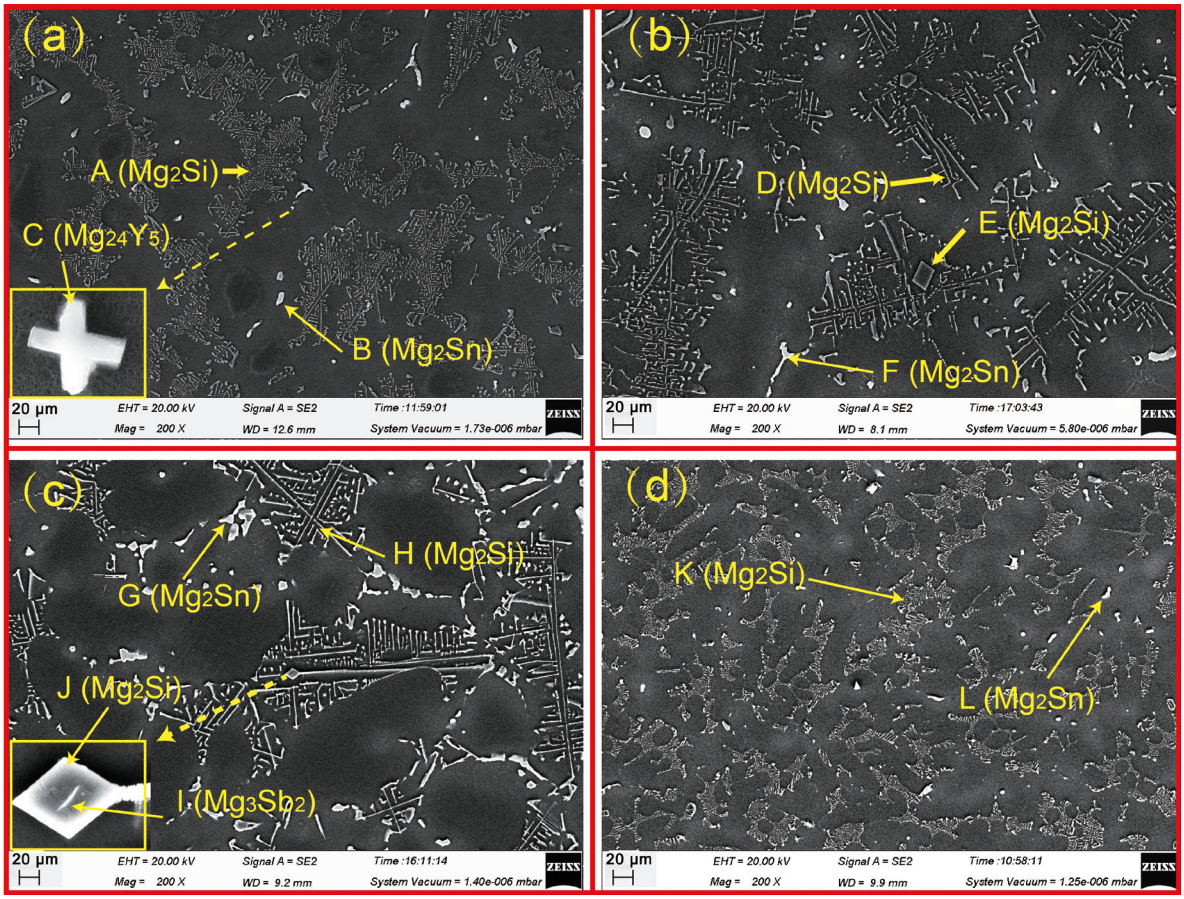

Fig. 5: SEM images of Mg-5Sn-1Si alloyswith 0.8wt.% Y (a), 0.3wt.% Bi (b), 0.9wt.% Sb (c), and 0.9wt.% Sr (d)

Table 3: EDS results of experimental alloys (wt.%)

Alloys	Position	Mg	Sn	Si	Y	Bi	Sb	Sr
Mg-5Sn-1Si-0.8Y	A	59.16	15.19	25.56	0.10	-	-	-
	B	32.52	63.97	3.33	0.18	-	-	-
	C	39.33	5.11	14.47	41.09	-	-	-
Mg-5Sn-1Si-0.3Bi	D	56.54	14.41	28.12	-	0.93		
	E	64.01	2.97	32.71	-	0.31	-	-
	F	36.26	59.62	2.13	-	1.99	-	-
Mg-5Sn-1Si-0.9Sb	G	31.66	59.06	0.55	-	-	8.73	
	H	55.47	7.72	22.33	-	-	14.47	-
	I	50.11	1.32	15.54	-	-	33.04	-
	J	53.20	5.50	26.24	-	-	15.03	-
Mg-5Sn-1Si-0.9Sr	K	61.23	9.40	28.59	-	-	-	0.78
	L	33.33	64.97	1.52	-	-	-	0.18

3.3 Tensile properties

The tensile properties of the studied alloys are shown in Fig. 6. The ultimate tensile strength (UTS) and elongation to failure of Mg-5Sn-1Si alloy under room temperature are 87 MPa and 4%, respectively. The UTS is 96 MPa for Mg-5Sn-1Si-0.8Y alloy, 108 MPa for Mg-5Sn-1Si-0.3Bi alloy, 117 MPa for Mg-5Sn-1Si-0.9Sb alloy and 123 MPa for Mg-5Sn-1Si-0.9Sr alloy, indicating that adding trace elements can improve the tensile properties of the Mg-5Sn-1Si alloy. The reasons for the improvement of the tensile properties of the modified alloys are ascribed to the grain refinement and modification of the Mg_2Si phase by adding the trace elements (Y, Bi, Sb and Sr). On the one hand, according to the Hall-Patch formula, grain refinement is very effective in improving the mechanical performance of magnesium alloy. On the other hand, the coarse Chinese script Mg_2Si has a detrimental effect on the tensile properties of Mg-Si alloys. The detrimental effect is related to the micro-cracks nucleated at the keen-edged corners of α-Mg/Mg_2Si interfaces. The keen-edged corners are the stress concentration areas. Hence, Mg-5Sn-1Si alloy has poor tensile properties. However, after adding trace elements to Mg-5Sn-1Si alloy, the coarse Chinese script Mg_2Si of the modified alloys is refined and then the micro-crack nucleation tendency of the modified Mg_2Si phase decreases. Therefore, the tensile properties of the modified alloys are improved. Besides, it can be observed that the Mg-5Sn-1Si-0.9Sr alloy has the best strengths. Based on the previous discussion of microstructure, Sr has the best refinement effect among the above four alloying elements. Apparently, the tensile properties of the investigated alloys are consistent with the microstructure observation.

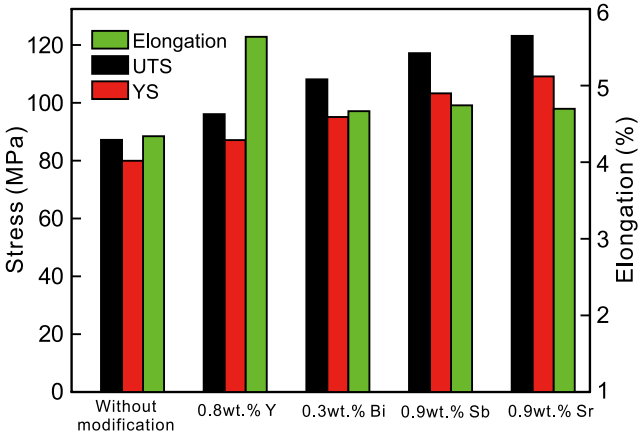

Fig. 6: Tensile properties of Mg-5Sn-1Si alloys modified with different elements

3.4 Discussion

Generally, grain refinement in cast Mg alloys can be achieved through micro-alloying. The refinement is realized by promotion of nucleation rate by manually adding or in situ forming particles, or by restriction of crystal growth by constitutional supercooling, or by both [2]. In the present study, since the solubility of each element of Y, Bi, Sb and Sr in α-Mg is in trace amount, and the equilibrium partition coefficient of each element is very small, these elements will definitely enrich in the front of the growing crystals through segregation during solidification. The enrichment inevitably results in the change of the crystals' growing environment. If the composition at the site of the growing front can meet the conditional requirement for a new phase to form, the new phase in turn can be as the nucleus to other phases, such as

Mg_3Sb_2 in Mg-5Sn-1Si-0.9Sb alloy can be as the nucleus of Mg_2Si. If the composition at the growing front cannot meet the conditional requirement for a new phase to form, the solute undercooling is beneficial to grain refinement.

It is now generally accepted that solute undercooling (ΔT) during solidification process and solute segregation [(quantified by the growth restriction factor (GRF)] [34] are critical in determining the final grain size and distribution of the second phase of as-cast magnesium alloys. In order to describe the impact of ΔT on as-cast grain size, a correlative growth restriction factor (GRF) or Q value is widely used. The Q_{total} value is simply expressed as:

$$Q_{total} = \Sigma m_i C_{0,i}(k_i - 1) \quad (1)$$

where m_i is the slope of the liquidus, $C_{0,i}$ the initial composition of the alloy, and k_i the equilibrium partition coefficient of the solute element [35-38]. A greater Q_{total} value means a higher ΔT ahead of the growing dendrite and will result in grain refinement. The Q values of the modification elements used in this study have been calculated with a simplified Mg-M binary system (where M represents the modified element) [35] and are listed in Table 4.

Table 4: Q values for solute elements [35]

Elements	m	k	$Q = m(k-1)$	System
Sn	-2.41	0.39	1.47	Mg-Sn eutectic
Si	-9.25	0	9.25	Mg-Si eutectic
Y	-3.40	0.50	1.70	Mg-Y eutectic
Bi	-1.814	0.145	1.551	Mg-Bi eutectic
Sb	-0.53	0	0.53	Mg-Sb eutectic
Sr	-3.53	0.006	3.51	Mg-Sr eutectic

The Q_{total} values of the modified alloys are calculated according to Eq. (1) and are listed in Table 5. Therefore, from the view point of GRF, Mg-5Sn-1Si-0.9Sr alloy has the largest Q_{total} value, so Sr is the most effective grain refinement element among the studied ones. The calculated result is also in good agreement with the microstructures of the alloys in Fig. 4. The Q_{total} values for Mg-5Sn-1Si-0.3Bi and Mg-5Sn-1Si-0.9Sb alloys are approximately the same (17.06 for Mg-5Sn-1Si-0.3Bi, and 17.07 for Mg-5Sn-1Si-0.9Sb); however, by comparing the microstructure and mechanical properties of Mg-5Sn-1Si-0.3Bi and Mg-5Sn-1Si-0.9Sb alloys, it is found that Mg-5Sn-1Si-0.9Sb alloy has much finer microstructure and better properties. The reason is related to the heterogeneous nuclei of Mg_3Sb_2 particles [Fig. 5(c)]. As a result, Mg-5Sn-1Si-0.9Sb alloy has finer microstructure, as shown in Fig. 4(c). Mg-5Sn-1Si-0.8Y alloy has a greater Q_{total} value than Mg-5Sn-1Si-0.3Bi and Mg-5Sn-1Si-0.9Sb. According to the GRF mechanism, Mg-5Sn-1Si-0.8Y alloy could have finer microstructure and better performance than Mg-5Sn-1Si-0.3Bi and Mg-5Sn-1Si-0.9Sb alloys. However, it can be observed that Mg-5Sn-1Si-0.8Y alloy has a much coarser grain and microstructure than Mg-5Sn-1Si-0.3Bi and Mg-5Sn-1Si-0.9Sb alloys, indicating that the GRF mechanism is not enough to explain the modification and refinement of Mg_2Si phase in the Mg-5Sn-1Si-0.8Y alloy. Besides the GRF mechanism, ΔT is also a very pivotal factor for the microstructural refinement of engineering alloys [39].

Table 5: Q_{total} values for different modified alloys

Alloys	Q_{total}
Mg-5Sn-1Si-0.8Y	17.96
Mg-5Sn-1Si-0.3Bi	17.06
Mg-5Sn-1Si-0.9Sb	17.07
Mg-5Sn-1Si-0.9Sr	19.76

According to classic solidification theory, the relationship between critical nucleus radius (r^*) and ΔT is given by [40]:

$$r^* = 2\delta/\Delta G_r = 2\delta T_m/L_m\Delta T \quad (2)$$

where ΔG_r is the variation of volume free energy, δ the interfacial energy of the unit surface area, $\Delta T = T_m - T_l$, T_m the equilibrium crystallizing temperature, T_l the onset crystallizing temperature, and L_m the crystallizing latent heat. According to Eq. (2), with decreasing T_l, the critical nucleus radius r^* decreases, then the nucleation energy of crystal nucleus reduces and the nucleation probability increases, and then results in grain refinement. In order to study the effect of ΔT on microstructures, the DSC was performed. Figure 7 shows the DSC curves of the experimental alloys. Mg-5Sn-1Si magnesium alloy has three endothermic peaks. According to Mg-Si, Mg-Sn and Mg-Sn-Si phase diagrams, it can be speculated the crystallization onset temperature of the primary α-Mg of the alloy is at about 648.9 °C and the eutectic reaction temperature is about 637.1 °C. After adding modified elements into Mg-5Sn-1Si magnesium alloy, the crystallization onset temperatures of the Mg-5Sn-1Si-0.8Y, Mg-5Sn-1Si-0.3Bi, Mg-5Sn-1Si-0.9Sb and Mg-5Sn-1Si-0.9Sr alloys decrease to 646.6 °C, 641.3 °C, 641.1 °C and 637.4 °C, and the crystallization eutectic reaction temperatures of the modified alloys decrease to 636.9 °C, 635.3 °C, 634.8 °C and 631 °C, respectively. Apparently, adding Y, Bi, Sb and Sr elements into Mg-5Sn-1Si increases ΔT and promotes the refinement of solidification microstructure. The onset crystallizing temperature

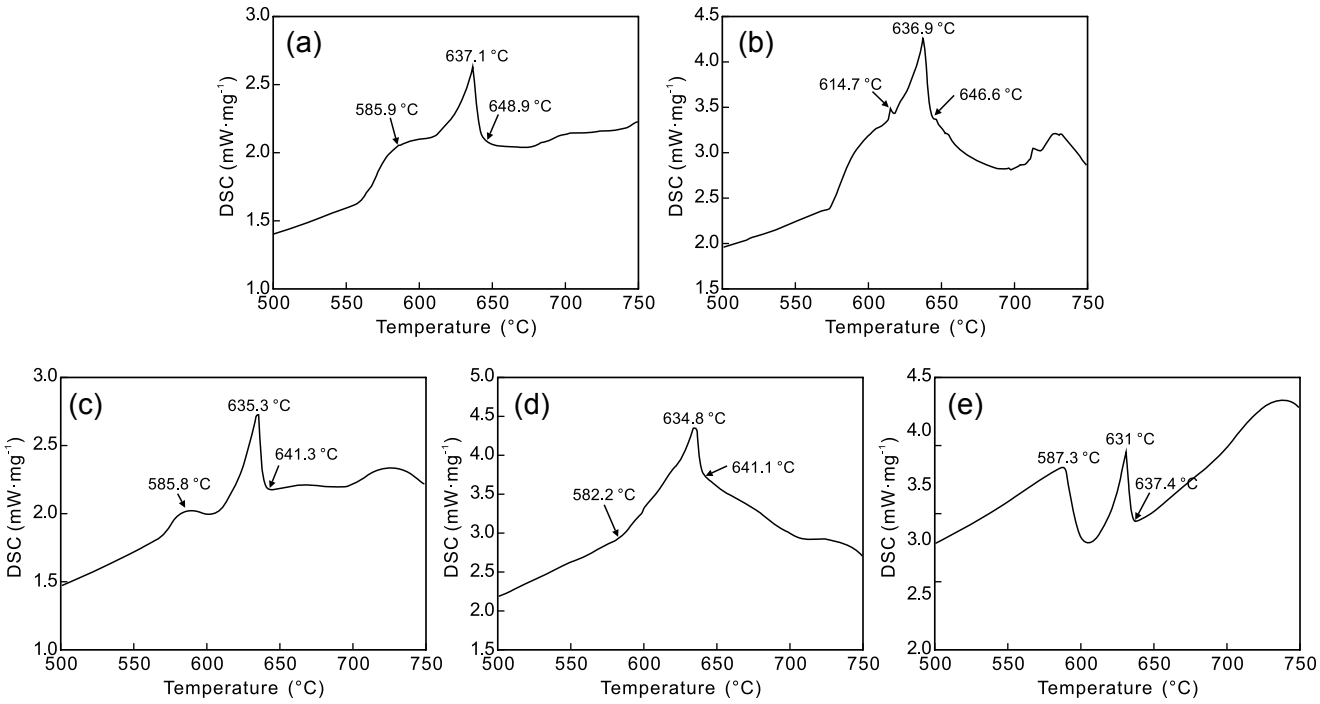

Fig. 7: DSC heating curves of experimental alloys: (a) Mg-5Sn-1Si alloy; (b) Mg-5Sn-1Si-0.8Y alloy; (c) Mg-5Sn-1Si-0.3Bi alloy; (d) Mg-5Sn-1Si-0.9Sb alloy; (e) Mg-5Sn-1Si-0.9Sr alloy

(T_1) of Mg-5Sn-1Si-0.8Y alloy is higher than that of Mg-5Sn-1Si-0.3Bi and Mg-5Sn-1Si-0.9Sb alloys. According to Eq. (2), the ΔT of Mg-5Sn-1Si-0.8Y alloy is smaller than that of the Mg-5Sn-1Si-0.3Bi and Mg-5Sn-1Si-0.9Sb alloy. Hence, the critical nucleus radius r^* increases, then the nucleation energy of crystal nucleus increases and the nucleation probability decreases. Finally, the Mg-5Sn-1Si-0.8Y alloy shows a much coarser grain size and microstructure. At the same time, Mg-5Sn-1Si-0.9Sr alloy has the lowest crystallization onset temperature. According to Eq. (2), with the decreasing of T_1, the critical nucleus radius r^* decreases, then the nucleation energy of crystal nucleus reduces and the nucleation probability increases, which would result in grain and precipitate refinement. Hence, has the finest microstructure.

Therefore, the refinement mechanism of Y, Bi and Sr elements on Mg-5Sn-1Si magnesium alloy can be explained by both the difference of GRF and the undercooling. For Mg-5Sn-1Si-0.9Sb alloy, the heterogeneous nuclei of Mg_3Sb_2 phase is the main reason for refinement.

4 Conclusions

In this study, the microstructures and tensile properties of as-cast Mg-5Sn-1Si magnesium alloy modified with trace elements Y, Bi, Sb and Sr are investigated and compared. The following conclusions can be drawn:

(1) The microstructure of as-cast Mg-5Sn-1Si alloy consists of α-Mg, Mg_2Si, Mg_2Sn and $Mg_2(Si_xSn_{1-x})$ phases. After adding trace elements of Y, Bi, Sb and Sr into Mg-5Sn-1Si magnesium alloy, $Mg_{24}Y_5$, Mg_3Bi_2, Mg_3Sb_2 and Mg_2Sr phases are precipitated, respectively.

(2) Adding 0.8wt.% Y, 0.3wt.% Bi, 0.9wt.% Sb or 0.9wt.% Sr elements into Mg-5Sn-1Si magnesium alloy can refine α-Mg grain and Chinese script-shaped Mg_2Si. Sr has the most refinement efficiency and Mg-5Sn-1Si-0.9Sr alloy has the most refined microstructure with a grain size of 74 μm, and the highest tensile strength of 123 MPa.

(3) The refinement mechanism of Y, Bi and Sr elements on Mg-5Sn-1Si magnesium alloy can be explained by the growth restriction factors and the solute undercooling. For Mg-5Sn-1Si-0.9Sb alloy, the heterogeneous nuclei of Mg_3Sb_2 phase is the main reason for the refinement of the grain and second phases.

Acknowledgements

The authors are grateful for the financial support by the National Natural Science Foundation of China (Nos.: 51571086 and 51271073) and the financial support from the Natural Science Foundation of Henan Polytechnic University (No.: B2010-20).

References

[1] Yang M P, Pan F S, Shen J, et al. Comparison of Sb and Sr on modification and refinement of Mg_2Si phase in AZ61-0.7Si magnesium alloy. Transactions of Nonferrous Metals Society of China, 2009, 19(2): 287–292.

[2] Ali Y, Qiu D, Jiang B, et al. Current research progress in grain refinement of cast magnesium alloys: A review article. Journal of Alloys and Compounds, 2015, 619: 639–651.

[3] Jung J H, Kang D H, Park W, et al. Thermodynamic modeling of the Mg-Si-Sn system. Calphad, 2007, 31(2): 192–200.

[4] Yu Z P, Yan Y H, Yao J, et al. Effect of tensile direction on mechanical properties and microstructural evolutions of rolled Mg-Al-Zn-Sn magnesium alloy sheets at room and elevated temperatures. Journal of Alloys and Compounds, 2018, 744: 211–219.
[5] Zhang W L, Li X F, Ding D Y, et al. Microstructure and mechanical properties of Mg_2Si/AZ91 composites in situ synthesized by using silica fume as the Si source. Journal of Materials Engineering and Performance, 2018, 27(10): 5300–5311.
[6] Dixit N, Xie K Y, Hemker K J, et al. Microstructural evolution of pure magnesium under high strain rate loading. Acta Materialia, 2015, 87: 56–67.
[7] Zhu S M, Abbott T B, Gibson M A, et al. The influence of minor Mn additions on creep resistance of die-cast Mg-Al-RE alloys. Materials Science and Engineering: A, 2017, 682: 535–541.
[8] Yu H S, Yang W P, Cui H P, et al. Microstructures and tensile properties of hot-extruded Mg-6Zn-*x*Ce (*x*=0, 0.6, 1.0, 2.0) alloys. Journal of Wuhan University of Technology, 2019, 34(1): 150–155.
[9] Yang W P, Guo X F. A high strength Mg-6Zn-1Y-1Ce alloy prepared by hot extrusion. Journal of Wuhan University of Technology-Mater. Sci. Ed., 2013, 28(2): 389–395.
[10] Baghani A, Khalilpour H, Miresmaeili S. The microstructure and impression creep behavior of cast Mg-4Sn-4Ca alloy. Materials Science and Engineering: A, 2016, 652: 365–369.
[11] Srinivasan A, Dieringa H, Mendis C L, et al. Creep behavior of Mg-10Gd-*x*Zn (*x*=2 and 6wt.%) alloys. Materials Science and Engineering: A, 2016, 649: 158–167.
[12] Kozlov A, Gröbner J, Schmid-Fetzer R. Phase formation in Mg-Sn-Si and Mg-Sn-Si-Ca alloys. Journal of Alloys and Compounds, 2011, 509(7): 3326–3337.
[13] Zhang J X, Wang H Y, Gao A H, et al. Study on thermodynamics basic and alloy phase evolution of Mg-Sn-Si magnesium alloy. Acta Physica Sinica, 2015, 6: 278-283. (In Chinese)
[14] Zhang M, Zhang W Z, Zhu G Z. The morphology and orientation of Mn_5Si_3 precipitates in a Mg-Sn-Mn-Si alloy. Materials Letters, 2008, 62(28): 4374–4376.
[15] Wang Y, Guo X F, Yang W P, et al. Morphology and properties of Mg_2Si and $Mg_2(Si_xSn_{1-x})$ reinforcements in magnesium alloys. Materials Science and Technology, 2017, 33(15): 1811–1818.
[16] Langelier B, Sha G, Korinek A, et al. The effects of microalloying on the precipitate microstructure at grain boundary regions in an Mg-Zn-based alloy. Materials & Design, 2017, 119: 290–296.
[17] Yang M B, Pan F S, Shen J, et al. Comparison of Sb and Sr on modification and refinement of Mg_2Si phase in AZ61-0.7Si magnesium alloy. Transactions of Nonferrous Metals Society of China, 2009, 19(2): 287–292.
[18] Tang S Q, Zhou J X, Tian C W, et al. Morphology modification of Mg_2Si by Sr addition in Mg-4%Si alloy. Transactions of Nonferrous Metals Society of China, 2011, 21(9): 1932–1936.
[19] Hou J, Li C, Liu X F. Nucleating role of an effective in situ Mg_3P_2 on Mg_2Si in Mg-Al-Si alloys. Journal of Alloys and Compounds, 2011, 509(3): 735–739.
[20] Guo E J, Ma B X, Wang L P. Modification of Mg_2Si morphology in Mg-Si alloys with Bi. Journal of Materials Processing Technology, 2008, 206(1–3): 161–166.
[21] Jiang Q C, Wang H Y, Wang Y, et al. Modification of Mg_2Si in Mg-Si alloys with yttrium. Materials Science and Engineering: A, 2005, 392(1–2): 130–135.
[22] Rajeshkumar R, Jayaraj J, Srinivasan A, et al. Investigation on the microstructure, mechanical properties and corrosion behavior of Mg-Sb and Mg-Sb-Si alloys. Journal of Alloys and Compounds, 2017, 691: 81–88.
[23] Liao L H, Zhang X Q, Wang H W, et al. Influence of Sb on damping capacity and mechanical properties of Mg_2Si/Mg-9Al composite materials. Journal of Alloys and Compounds, 2007, 430(1–2): 292–296.
[24] Yang M B, Shen J, Pan F S. Effect of Sb on microstructure of semi-solid isothermal heat-treated AZ61-0.7Si magnesium alloy. Transactions of Nonferrous Metals Society of China, 2009, 19(1): 32–39.
[25] Wang L P, Guo E J, Ma B X. Modification effect of lanthanum on primary phase Mg_2Si in Mg-Si alloys. Journal of Rare Earths, 2008, 26(1): 105–109.
[26] Hu J L, Tang C P, Zhang X M, et al. Modification of Mg_2Si in Mg-Si alloys with neodymium. Transactions of Nonferrous Metals Society of China, 2013, 23(11): 3161–3166.
[27] Ye L Y, Hu J L, Tang C P, et al. Modification of Mg_2Si in Mg-Si alloys with gadolinium. Materials Characterization, 2013, 79: 1–6.
[28] Wang H Y, Wang W, Zha M, et al. Influence of the amount of KBF_4 on the morphology of Mg_2Si in Mg-5Si alloys. Materials Chemistry and Physics, 2008, 108(2–3): 353–358.
[29] Liu H M, Chen Y G, Tang Y B, et al. The microstructure, tensile properties, and creep behavior of as-cast Mg-(1–10)%Sn alloys. Journal of Alloys and Compounds, 2007, 440(1–2): 122–126.
[30] Ma J, Guo X F, Wang Y, et al. Influence of trace Y on microstructure of Mg-5Sn-1Si magnesium alloy. Hot Working Technology, 2019, 48(12): 34–39. (In Chinese)
[31] Yan H, Hu Y, Wu X Q, et al. Influence of Sb modification on microstructures and mechanical properties of Mg_2Si/AM60 composites. Transactions of Nonferrous Metals Society of China, 2010, 20(S2): 411–415.
[32] Wang Y, Guo X F. Heterogeneous nucleation of Mg_2Si and $Mg_2(Si,Sn)$ on Mg_3Sb_2 nucleus in Mg Containing Si alloys. Materials Chemistry & Physics, 2018.
[33] Cong M Q, Li Z Q, Liu J S, et al. Effect of Sr on microstructure, tensile properties and wear behavior of as-cast Mg-6Zn-4Si alloy. Materials & Design, 2014, 53: 430–434.
[34] Xu Y J, Zhao D D, Li Y J. A Thermodynamic Study on the effect of solute on the nucleation driving force, solid-liquid interfacial energy, and grain refinement of Al alloys. Metallurgical and Materials Transactions A, 2018, 49(5): 1770–1781.
[35] David H S, Ma Q, et al. Grain refinement of magnesium alloys. Metallurgical & Materials Transactions A, 2005, 36, 1669–1679.
[36] Schmid-Fetzer R, Kozlov A. Thermodynamic aspects of grain growth restriction in multicomponent alloy solidification. Acta Materialia, 2011, 59(15): 6133–6144.
[37] Quested T E, Dinsdale A T, Greer A L. Thermodynamic modelling of growth-restriction effects in aluminium alloys. Acta Materialia, 2005, 53(5): 1323–1334.
[38] Men H, Fan Z. Effects of solute content on grain refinement in an isothermal melt. Acta Materialia, 2011, 59(7): 2704–2712.
[39] Yang M B, Pan F S, Cheng R J, et al. Comparison about effects of Sb, Sn and Sr on as-cast microstructure and mechanical properties of AZ61-0.7Si magnesium alloy. Materials Science and Engineering: A, 2008, 489(1–2): 413–418.
[40] Zhao P, Wang Q D, Zhai C Q, et al. Effects of strontium and titanium on the microstructure, tensile properties and creep behavior of AM50 alloys. Materials Science and Engineering: A, 2007, 444(1–2): 318–326.